E-30-H-15

NAS 1.60 : 1615

COMPLETED

ORIGINAL

NASA Technical Paper 1615

Extension of Similarity Test Procedures to Cooled Engine Components With Insulating Ceramic Coatings

Herbert J. Gladden

MAY 1980

NASA

16

NASA Technical Paper 1615

Extension of Similarity Test Procedures to Cooled Engine Components With Insulating Ceramic Coatings

Herbert J. Gladden
Lewis Research Center
Cleveland, Ohio

National Aeronautics
and Space Administration

**Scientific and Technical
Information Office**

1980

SUMMARY

An analysis was made of the effects of material thermal conductivity on the thermal performance of air-cooled gas turbine components coated with a ceramic thermal-barrier material tested at reduced temperatures and pressures. Because of the complexity and expense of evaluating these components at actual engine conditions, prototype hardware is often evaluated at test conditions derived from established similarity constraints.

The results of this study show that neglecting the effects of material thermal conductivity, as is often done, can contribute significant errors to the results when metal-wall-temperature test data taken on a turbine vane are extrapolated to engine conditions. The error in metal temperature for an uncoated turbine vane is of opposite sign from the error for a ceramic-coated vane. A technique for correcting test data to engine conditions was developed. The correction technique was applied to an experimental vane-metal-temperature distribution obtained from similarity-derived test gas conditions (580 K and 7.5 atm) based on assumed typical turbofan engine gas conditions (1980 K and 30 atm). Corrections as great as a 9-percent increase in dimensionless wall temperature for uncoated turbine vanes and a 10-percent decrease for ceramic-coated vanes were needed for these conditions.

INTRODUCTION

Ceramic thermal-barrier coatings are being considered for the hot-section components of gas turbine engines as a supplement to the thermal protection provided by various air-cooling schemes. The thermal performance of some of these coated components is evaluated at reduced gas temperatures and pressures to avoid the complexity and expense of testing at actual engine gas conditions. However, extrapolating (scaling) these test results to engine conditions can lead to erroneous conclusions if the material thermal conductivity, in addition to the usual nondimensional groups, is not properly considered.

Several techniques exist that can be used to establish the reduced temperatures and pressures (refs. 1 to 3) necessary for testing turbine components at similarity conditions. The approach used in each reference is somewhat different, but the results and conclusions are basically the same. That is, the kinematic, dynamic, and thermal similarities of the gas and coolant can be maintained between test and engine conditions by preserving the equality of various dimensionless parameters such as the Reynolds, Mach, and

Prandtl numbers. These references also discuss the need to maintain material-thermal-conductivity similarity so that the thermal performance of the hardware will be similar at both test and engine conditions. The references show that the thermal conductivity effect is not significant for the materials and conditions they considered. However, cases where layers of a ceramic coating material are added to the basic component and where other types of high-temperature materials are used have not been fully analyzed.

This report combines the analyses of references 1 and 2 to form a method of scaling test data taken at reduced temperature and pressure to engine conditions. A method of calculating the error resulting from the inability to physically scale material thermal conductivity is also presented. The effects of similarity testing on vane thermal performance when a ceramic thermal-barrier coating is added to a turbine vane are discussed. The analysis is then applied to assumed conditions of an advanced gas turbine engine with a gas temperature and pressure of 1980 K and 30 atmospheres, respectively, and to similarity-derived test conditions of 590 K and 7.5 atmospheres.

The results are presented as an error between engine and test conditions when the same materials are used for both engine and scaled tests for various turbine airfoil cooling efficiencies. This error is shown for two thicknesses of a NASA thermal-barrier coating on a typical turbine airfoil material and for several typical airfoil materials without a ceramic coating. The method of correction is then applied to a typical turbine-vane temperature distribution obtained at a reduced gas temperature and pressure.

SYMBOLS

A	heat-transfer area
f	friction factor
h	heat-transfer coefficient
k	thermal conductivity
M	Mach number
N	number of ceramic coating layers
Nu	Nusselt number
Pr	Prandtl number
p	pressure
q	heat flux
R	gas constant
Re	Reynolds number

T	temperature
T*	$(T_{wo} - T_{ci})/(T_g - T_{ci})$
U	velocity
w	mass flow rate
x	surface distance
X, Y, Z	dimensionless geometric terms
Γ	function of specific-heat ratios
γ	specific-heat ratio
μ	viscosity
τ	wall or coating thickness; characteristic dimension
φ	cooling effectiveness, $(T_{ge} - T_{wo})/(T_{ge} - T_c)$

Subscripts:

c	coolant
ci	coolant inlet
e	engine
g	gas
ge	effective gas
t	test
u	uncoated condition
w	wall
wi	coolant side of metal wall
wo	gas side of metal wall
z	ceramic
z, n	n^{th} layer of ceramic
z, N	gas-side ceramic surface
z, 0	metal-ceramic interface
∞	free stream

Superscripts:

e	engine conditions
t	test conditions

ANALYSIS METHOD

Similarity

Differential similarity is used in reference 1 to determine many of the important dimensionless groups that must be considered when testing components at reduced (scaled) temperatures and pressures. The following dimensionless groups are shown to be important to the proper scaling of the component test:

$$X,\ Y,\ Z,\ Re,\ Pr,\ M_\infty,\ U_c/U_\infty,\ T_c/T_g,\ P_c/P_g,\ \mu_c/\mu_g,\ k_c/k_g,\ k_w/k_g \qquad (1)$$

plus radiation and turbulence terms. The first 11 dimensionless groups are sufficient to satisfy the geometric similarity of the apparatus and the kinematic, dynamic, and thermal similarities of the gas and coolant environments. The last term (k_w/k_g) concerns the thermal similarity of the material and can, in general, only be satisfied by using different materials in the engine and in the test hardware to maintain the ratio of material to gas thermal conductivity. Protytype hardware is commonly used in tests of engine components. The incompatibility of this usage with the requirement of material similarity is the reason for this report. The radiation and turbulence terms are complex terms that are also difficult or impossible to scale between the engine and test conditions. These terms are not considered herein.

Physical insight is used in references 2 and 3 to determine the parameters that must be considered to maintain the similarity between engine and test conditions. The conclusions of these references are quite similar to those of reference 1. That is, the Reynolds, Prandtl, and Mach numbers are sufficient to ensure dynamic, kinematic, and thermal similarity of the gas and coolant. Geometric similarity is maintained by using the engine component hardware. The following equations from references 2 and 3 establish the relationship between the engine and test conditions for both the hot gas and the coolant. These equations are based on an equality of momentum-thickness Reynolds number and Mach number between the gas conditions of the engine and similarity tests. In addition, an equality of the coolant Reynolds number is assumed.

$$\frac{p_g^t}{p_g^e}\frac{\mu_g^e}{\mu_g^t}\sqrt{\frac{RT_g^e}{RT_g^t}}\frac{\Gamma_g^t}{\Gamma_g^e}=1 \tag{2}$$

where

$$\Gamma_g=\sqrt{\gamma}\left(\frac{2}{\gamma+1}\right)^{(\gamma+1)/2(\gamma-1)}$$

$$\left(\frac{w_c}{w_g}\right)^t=\left(\frac{w_c}{w_g}\right)^e \tag{3}$$

$$\left(\frac{\mu_c}{\mu_g}\right)^t=\left(\frac{\mu_c}{\mu_g}\right)^e \tag{4}$$

Maintaining similarity between test and engine conditions is necessary for duplicating the thermal performance of test components. For air-cooled turbine vanes the temperature distribution around the vane airfoil periphery is generally sought by these tests. Reference 2 has shown that airfoil temperatures at engine conditions can be predicted from test results by a dimensionless temperature-difference ratio. This ratio $(T_{ge} - T_{wo})/(T_{ge} - T_c)$, which is also called the cooling effectiveness φ, is based on a one-dimensional heat balance that assumes heat flow only from the gas to the coolant by convection and conduction.

A representative cross-sectional schematic of a cooled turbine component with multiple layers of a ceramic coating on a metal substrate is shown in figure 1. The component temperature is assumed to be known at the metal-ceramic interface. The following one-dimensional equations can be written by neglecting lateral heat conduction in the component and radiation heat transfer between the component and the surrounding environment:

$$q_g = q_{z,n} = q_w = q_c \tag{5}$$

where

$$q_g = h_g A_g (T_{ge} - T_{z,N}) = \frac{Nu_g A_g (T_{ge} - T_{z,N}) k_g}{\tau_g} \tag{6}$$

$$q_{z,n} = \frac{k_{z,n} A_{z,n} (T_{z,n} - T_{z,n-1})}{\tau_{z,n}} \quad \text{for } n = 1 \text{ to } N \tag{7}$$

$$q_w = \frac{k_w A_w}{\tau_w} (T_{z,0} - T_{wi}) = \frac{k_w A_w}{\tau_w} (T_{wo} - T_{wi}) \tag{8}$$

$$q_c = h_c A_c (T_{wi} - T_c) = \frac{Nu_c A_c (T_{wi} - T_c) k_c}{\tau_c} \tag{9}$$

(The metal-ceramic interface temperature $T_{z,0}$ is also the gas-side metal temperature T_{wo}.) The inlet total gas and coolant temperature values can be substituted for local values (ref. 4), and equations (5) to (9) can then be combined to obtain the following dimensionless form. It is also assumed that the heat-transfer areas through the airfoil are equal (no curvature).

$$T_g - T_{wo} = \frac{q_g \tau_g}{Nu_g k_g} + \frac{q_{z,1} \tau_{z,1}}{k_{z,1}} + \frac{q_{z,2} \tau_{z,2}}{k_{z,2}} + \ldots + \frac{q_{z,N} \tau_{z,N}}{k_{z,N}} \tag{10}$$

$$T_{wo} - T_{ci} = \frac{q_w \tau_w}{k_w} + \frac{q_c \tau_c}{Nu_c k_c} \tag{11}$$

$$\frac{T_g - T_{wo}}{T_g - T_{ci}} = \varphi = \frac{1 + \sum_{n=1}^{N} \left(\frac{Nu_g k_g \tau_{z,n}}{k_{z,n} \tau_g} \right)}{1 + \left(\frac{Nu_g}{Nu_c} \right) \left(\frac{k_g}{k_c} \right) \left(\frac{\tau_c}{\tau_g} \right) + \frac{Nu_g k_g}{k_w} \frac{\tau_w}{\tau_g} + \sum_{n=1}^{N} \left(\frac{Nu_g k_g}{k_{z,n}} \right) \left(\frac{\tau_{z,n}}{\tau_g} \right)} \tag{12}$$

where n denotes the layers of ceramic coating on the metal substrate. A vane without ceramic coating can be represented by equations (6), (8), and (9), where $T_{z,N}$ in equation (6) is replaced by T_{wo}:

$$\frac{T_g - T_{wo}}{T_g - T_{ci}} = \varphi = \left(1 + \frac{Nu_g k_g \tau_c}{Nu_c k_c \tau_g} + \frac{Nu_g k_g \tau_w}{k_w \tau_g}\right)^{-1} \tag{13}$$

Equations (12) and (13) show that for the model cooling effectiveness φ to be directly applicable it is necessary to have Nusselt number similarity. Since heat-transfer results follow the form $Nu = f(Re, Pr)$, Reynolds and Prandtl number similarity assures achieving the Nusselt number similarity required in equations (12) and (13). In addition, equality of the thermal conductivity ratios k_g/k_w and $k_g/k_{z,n}$ must be maintained if total similarity of the cooling effectiveness is to be maintained between test and engine conditions. That is generally not possible with most component materials.

Cooling Effectiveness Correction

The inability to maintain equality of the thermal conductivity ratios can lead to significant errors when using the test data directly to predict component temperatures at engine conditions. The magnitude of this error can be determined by calculating the total derivative of equations (12) and (13) with respect to these variables.

$$d\varphi = \sum_{n=1}^{N} \left[\frac{\partial \varphi}{\partial\left(\frac{k_g}{k_{z,n}}\right)}\right] d\left(\frac{k_g}{k_{z,n}}\right) + \left[\frac{\partial \varphi}{\partial\left(\frac{k_g}{k_w}\right)}\right] d\left(\frac{k_g}{k_w}\right) \tag{14}$$

The specific case of a turbine vane with a single layer of ceramic coating material reduces the summation to one term. The first partial derivative in equation (14) becomes

$$\frac{\partial \varphi_z}{\partial\left(\frac{k_g}{k_z}\right)} = \frac{\left[\left(\frac{Nu_g}{Nu_c}\right)\left(\frac{\tau_c}{\tau_g}\right)\left(\frac{k_g}{k_c}\right) + Nu_g\left(\frac{\tau_w}{\tau_g}\right)\left(\frac{k_g}{k_w}\right)\right] Nu_g\left(\frac{\tau_z}{\tau_g}\right)}{\left[1 + \left(\frac{Nu_g}{Nu_c}\right)\left(\frac{\tau_c}{\tau_g}\right)\left(\frac{k_g}{k_c}\right) + Nu_g\left(\frac{\tau_w}{\tau_g}\right)\left(\frac{k_g}{k_w}\right) + Nu_g\left(\frac{\tau_z}{\tau_g}\right)\left(\frac{k_g}{k_z}\right)\right]^2} \tag{15}$$

The second partial derivative in equation (14) becomes

$$\frac{\partial \varphi_z}{\partial \left(\frac{k_g}{k_w}\right)} = - \frac{\left[1 + Nu_g \left(\frac{\tau_z}{\tau_g}\right)\left(\frac{k_g}{k_z}\right)\right] Nu_g \left(\frac{\tau_w}{\tau_g}\right)}{\left[1 + \left(\frac{Nu_g}{Nu_c}\right)\left(\frac{\tau_c}{\tau_g}\right)\left(\frac{k_g}{k_c}\right) + Nu_g \left(\frac{\tau_w}{\tau_g}\right)\left(\frac{k_g}{k_w}\right) + Nu_g \left(\frac{\tau_z}{\tau_g}\right)\left(\frac{k_g}{k_z}\right)\right]^2} \tag{16}$$

Finally, combining equations (15) and (16) and simplifying give the correction factor for a ceramic-coated turbine vane as

$$\Delta\varphi_{z,e-t} = \varphi_{z,t}^2 \frac{\left(\frac{1 - \varphi_{z,t}}{\varphi_{z,t}}\right)\left(Nu_g \frac{\tau_z}{\tau_g}\right)_t \Delta\left(\frac{k_g}{k_z}\right)_{e-t} - \left(Nu_g \frac{\tau_w}{\tau_g}\right)_t \Delta\left(\frac{k_g}{k_w}\right)_{e-t}}{\left[1 + Nu_g \left(\frac{\tau_z}{\tau_g}\right)\left(\frac{k_g}{k_z}\right)\right]_t} \tag{17}$$

where

$$\Delta\left(\frac{k_g}{k_z}\right)_{e-t} = \left(\frac{k_g}{k_z}\right)_e - \left(\frac{k_g}{k_z}\right)_t$$

and

$$\Delta\left(\frac{k_g}{k_w}\right)_{e-t} = \left(\frac{k_g}{k_w}\right)_e - \left(\frac{k_g}{k_w}\right)_t$$

The correction factor for an uncoated turbine vane is written as follows:

$$\Delta\varphi_{u,e-t} = - \varphi_{u,t}^2 \left(Nu_g \frac{\tau_w}{\tau_g}\right)_t \Delta\left(\frac{k_g}{k_w}\right)_{e-t} \tag{18}$$

Finally, the cooling effectiveness at engine conditions can be defined as the cooling effectiveness at test conditions plus the correction factor.

$$\varphi_e = \varphi_t + \Delta\varphi_{e-t} \tag{19}$$

All the terms in these equations for the correction factors are known or can be calculated. The gas-side heat-transfer coefficient can be calculated by the method in which the user has most confidence in modeling his experiment. The turbulent flat-plate correlation is used herein. For the uncoated turbine vane

$$h_g = 0.029\left(\frac{k_g}{x}\right)Re^{0.8}Pr^{1/3} \tag{20}$$

Since the surface of the ceramic-coated vane may be rougher than the surface of the uncoated vane, the heat-transfer coefficient in equation (9) can be increased by the method of reference 5.

$$\frac{Nu}{Nu_{smooth}} = \left(\frac{f}{f_{smooth}}\right)^{1/2} \tag{21}$$

The gas and coolant thermodynamic and transport properties are taken from reference 6; the metal and ceramic thermal conductivity values are taken from references 7 and 8, respectively.

RESULTS AND DISCUSSION

The similarity relationship of turbine inlet gas temperature and pressure between engine and test conditions as expressed by equation (2) is shown in figure 2. One point on the curve is for a typical advanced turbofan engine with a turbine inlet temperature and pressure of 1980 K and 30 atmospheres, respectively. The inlet coolant temperature for this engine is 730 K. Choosing either a test gas temperature or pressure fixes the other and also fixes all other parameters that satisfy the similarity relationships discussed in the section Analysis Method. The test conditions selected for discussion were based on the capabilities of the four-vane cascade discussed in reference 2. The test gas temperature and pressure are 580 K and 7.5 atmospheres, respectively, as shown in figure 2. The inlet coolant temperature for these similarity conditions is 260 K.

The calculated effects of reduced temperature on metal wall and ceramic thermal conductivities between test and engine conditions is shown in figure 3 as a ratio of the thermal conductivity parameters $\left(k_g/k_w\right)_t/\left(k_g/k_w\right)_e$. The subscript w refers to either the metal or the ceramic coating. Evaluating this ratio at the assumed engine and test conditions and a cooling effectiveness of 0.6 shows that, of several typical materials used in airfoil fabrication, this ratio is least sensitive for IN-100 and is most sensitive for MAR M-302 to a reduction in temperature level. The ceramic thermal-barrier coating material zirconium dioxide (ZrO_2) is also very sensitive. The large deviations from unity at test conditions can contribute significant errors when reduced temperature and pressure test data are used directly to predict airfoil metal temperatures at engine conditions.

The correction factor $\Delta\varphi$ calculated for the engine and test conditions by using equations (17) and (18) is shown in figure 4 for a range of φ that reflects variations in coolant flow rate. This figure shows the correction required for the thermal conductivity of uncoated vanes of MAR M-509 and MAR M-302 and of ceramic coated vanes of MAR M-302 with 0.025- and 0.050-centimeter thicknesses of the ceramic ZrO_2.

The important point to note is that corrections for the uncoated vanes are always negative but corrections for the ceramic-coated vane increase to a maximum and then decrease. Within the range of interest the correction factors for the coated vanes are positive. Figure 4 shows that corrections of as much as 0.08 and -0.06 in the value of φ for ceramic-coated vanes and uncoated vanes, respectively, are required. Thus wall temperatures predicted for engine conditions without this correction would be too high for ceramic-coated vanes and too low for uncoated vanes.

The correction factors of figure 4 are converted in figure 5 to a percentage of a dimensionless wall temperature parameter, $T^* = 1 - \varphi$, for uncoated MAR M-302 and for MAR-M-302 with a typical coating thickness of 0.025 centimeter. The correction in the dimensionless wall temperature parameter is as much as 9 percent for the uncoated vane and -10 percent for the ceramic-coated vane.

An example of the correction technique applied to the measured metal temperature distributions around the peripheries of a coated and an uncoated vane is shown in figure 6, where the test conditions and assumed engine conditions are those shown in figure 2. The corrected metal temperature for the uncoated vane is higher than the experimental temperature; the corrected metal temperature for the ceramic-coated vane is lower than the experimental temperature. The correction of the data properly accounts for the insulating benefits of the ceramic coating. The results of the temperature correction are particularly apparent on the suction surface near the leading edge, where the uncorrected data show little or no insulating benefits for the coating but the corrected data show substantial benefits.

CONCLUSIONS

The effects of similarity testing on the thermal performance of air-cooled turbine vanes were analyzed for both ceramic-coated and uncoated vanes. Based on the results of this study a method was developed to account for the inability to maintain similarity of material thermal conductivity when conducting heat-transfer tests at other than engine conditions. The following conclusions were drawn from this study based on conditions examined:

1. The wall temperatures predicted directly from similarity tests of a typical uncoated, air-cooled turbine vane will be lower than temperatures at actual engine conditions unless variations in material thermal conductivity are taken into account. The error can be as great as 9 percent of the dimensionless wall temperature parameter.

2. When a ceramic thermal-barrier coating is added to an air-cooled turbine vane, the predicted metal wall temperatures will be higher than temperatures at actual engine conditions. This error is of opposite sign to the uncoated-vane error and can be as great as 10 percent of the dimensionless wall temperature parameter.

3. Directly comparing the similarity-test data results of a turbine vane with and without a ceramic coating and neglecting to correct for material-thermal-conductivity effects will show significantly poorer thermal protection by the coating than would actually occur at engine conditions.

Lewis Research Center,
National Aeronautics and Space Administration,
Cleveland, Ohio, February 5, 1980,
505-04.

REFERENCES

1. Sucec, James: Application of Differential Similarity to Finding Nondimensional Groups Important in Tests of Cooled Engine Components. NASA TM X-3484, 1977.

2. Gladden, Herbert J.; and Livingood, John N. B.: Procedure for Scaling of Experimental Turbine Vane Airfoil Temperatures from Low to High Gas Temperatures. NASA TN D-6510, 1971.

3. Colladay, Raymond S.; and Stepka, Francis S.: Similarity Constraints in Testing of Cooled Engine Parts. NASA TN D-7707, 1974.

4. Gladden, Herbert J.; Gauntner, Daniel J.; and Livingood, John N. B.: Analysis of Heat Transfer Tests of an Impingement-Convection- and Film-Cooled-Vane in a Cascade. NASA TM X-2376, 1971.

5. Kays, W. M.: Convection Heat and Mass Transfer. McGraw-Hill Book Co., Inc., 1966, p. 197.

6. Poferl, David J.; Svehla, Roger A.; and Lewandowski, Kenneth: Thermodynamic and Transport Properties of Air and the Combustion Products of Natural Gas and of ASTM A-1 with Air. NASA TN D-5452, 1969.

7. High Temperature, High Strength Nickel Base Alloys. The International Nickel Co., Inc., 1964.

8. Liebert, Curt H.; and Stepka, Francis S.: Industry Tests of NASA Ceramic Thermal-Barrier Coating. NASA TP-1425, 1979.

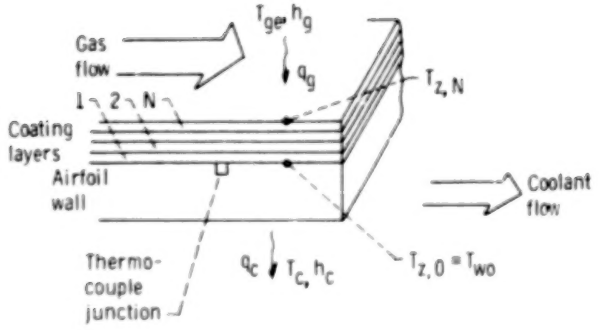

Figure 1. - One-dimensional heat-transfer model of airfoil wall with N layers of ceramic coating. Thermocouple junction located at interface of first layer of coating and metal wall.

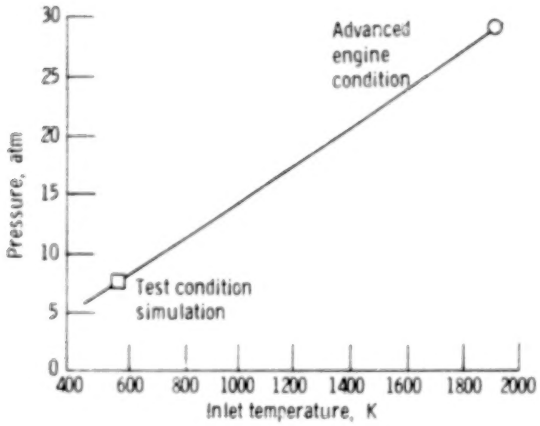

Figure 2. - Typical similarity curve for combustion-gas environment of an advanced turbofan engine.

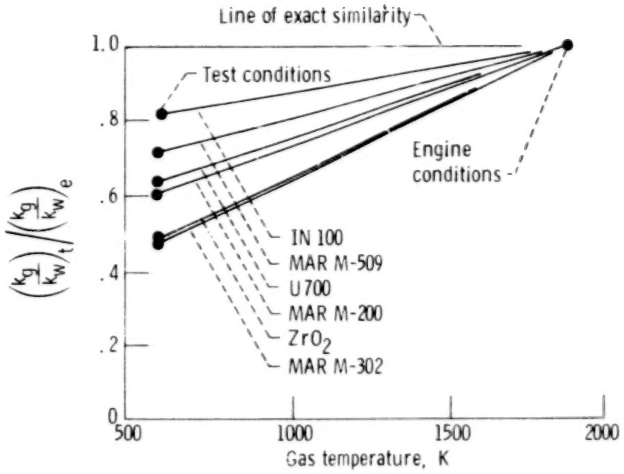

Figure 3. - Ratio of thermal conductivities between test and engine conditions for several typical high-temperature materials at a cooling effectiveness of 0.6.

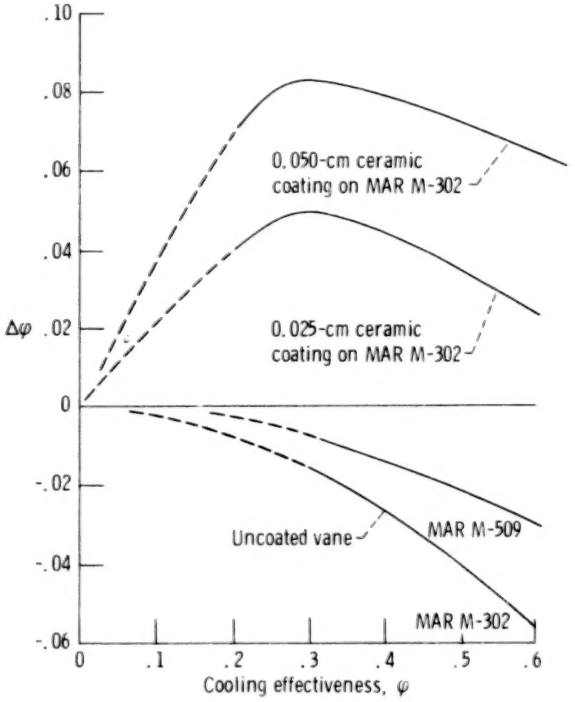

Figure 4. - Corrections for cooling effectiveness when scaling reduced-temperature test conditions to engine conditions.

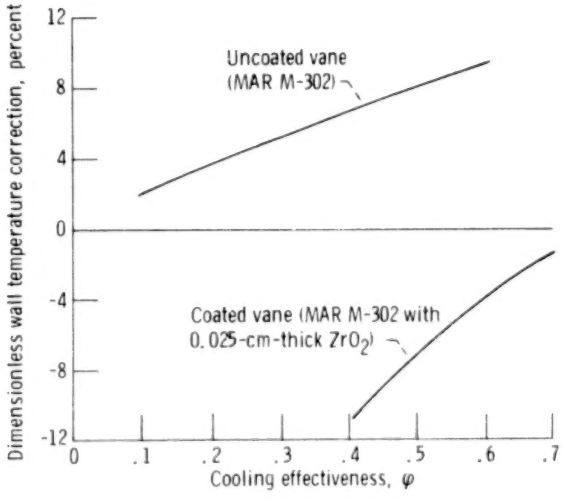
Uncoated vane (MAR M-302)
Coated vane (MAR M-302 with 0.025-cm-thick ZrO_2)
Dimensionless wall temperature correction, percent
Cooling effectiveness, φ

Figure 5. - Typical corrections for ceramic-coated and uncoated airfoils.

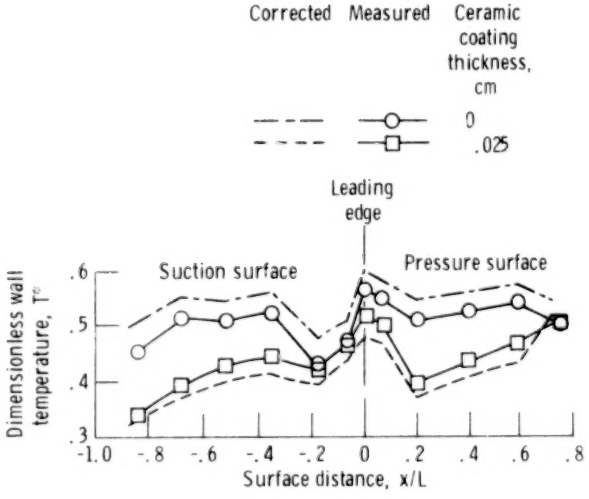

Figure 6. - Dimensionless metal temperature distributions at test vane midspan for ceramic-coated and uncoated vanes.

1. Report No.	2. Government Accession No.	3. Recipient's Catalog No.
NASA TP-1615		

4. Title and Subtitle	5. Report Date
EXTENSION OF SIMILARITY TEST PROCEDURES TO COOLED ENGINE COMPONENTS WITH INSULATING CERAMIC COATINGS	May 1980
	6. Performing Organization Code

7. Author(s)	8. Performing Organization Report No.
Herbert J. Gladden	E-337
	10. Work Unit No. 505-04

9. Performing Organization Name and Address	11. Contract or Grant No.
National Aeronautics and Space Administration Lewis Research Center Cleveland, Ohio 44135	
	13. Type of Report and Period Covered: Technical Paper

12. Sponsoring Agency Name and Address	14. Sponsoring Agency Code
National Aeronautics and Space Administration Washington, D.C. 20546	

15. Supplementary Notes

16. Abstract

Material thermal conductivity was analyzed for its effect on the thermal performance of air-cooled gas turbine components, both with and without a ceramic thermal-barrier material, tested at reduced temperatures and pressures. The analysis showed that neglecting the material thermal conductivity can contribute significant errors when metal-wall-temperature test data taken on a turbine vane are extrapolated to engine conditions. This error in metal temperature for an uncoated vane is of opposite sign from that for a ceramic-coated vane. A correction technique is developed for both ceramic-coated and uncoated components.

17. Key Words (Suggested by Author(s))	18. Distribution Statement
Similarity Heat transfer Gas turbines engines Turbine temperatures	Unclassified - unlimited STAR Category 34

19. Security Classif. (of this report)	20. Security Classif. (of this page)	21. No. of Pages	22. Price*
Unclassified	Unclassified	15	A02

* For sale by the National Technical Information Service, Springfield, Virginia 22161

NASA-Langley, 1980

90 %

50 %